

Institutional Analysis for Future Heat Wave Scenarios: Sandia National Laboratories California Site

Daniel L. Villa, PE

Member ASHRAE

ABSTRACT

Heat waves have catastrophic effects causing mortality, air quality loss, grid failures, infrastructure damage, and increases in electricity consumption. The literature indicates that heat waves are growing in intensity, duration, and frequency. This paper documents a heat wave study of the Sandia National Laboratories (SNL) California site. The analysis involves: 1) projection of a heat wave based on historical data and NEX-DCP30 climate projections, 2) Classification of peak electricity load points that represent the site on workdays, Fridays, and weekends 3) Regression of the peak load data to produce confidence bounds for the analysis, and 4) Calibration and projection of building energy models (BEMs) to the heat wave scenario. This approach worked well for the previous NM site analysis of meter data and 97 representative BEM's. For the CA site, the BEM calibration procedure was unsuccessful without individual BEM calibrations. Many of the 23 California BEM's required calibration at the building level rather than for the entire site. This was found to be due to many of the BEM's having significantly different electric demand profiles than their meter data whereas the NM BEM's were much more accurate. Unlike the NM site, the CA site did not distinguish Friday operations clearly and the associated K-mean cluster algorithm that worked for the NM site did not add value for the CA site. The regression analyses produced estimates of site-wide increases to daily peak loads with 95% confidence bounds that were much wider than the NM analysis. The CA site was found to have higher average peak load sensitivity of $1.07\%/\text{ }^{\circ}\text{C}$ ($0.59\%/\text{ }^{\circ}\text{F}$) in comparison to the NM site with $0.61\%/\text{ }^{\circ}\text{C}$ ($0.34\%/\text{ }^{\circ}\text{F}$). Even so, the larger sensitivity is counteracted by a milder projection for future heat waves from NEX-DCP30 downscaled climate projections. The expected heat wave maximum temperature of $45.1\text{ }^{\circ}\text{C}$ ($113.2\text{ }^{\circ}\text{F}$) did not even break the current record of $46.1\text{ }^{\circ}\text{C}$ ($115.0\text{ }^{\circ}\text{F}$) in Livermore, CA and only had total heating energy of $28\text{ }^{\circ}\text{C}\cdot\text{day}$ ($51\text{ }^{\circ}\text{F}\cdot\text{day}$) from baseline 2019 weather in comparison to NM's $38\text{ }^{\circ}\text{C}\cdot\text{day}$ ($68\text{ }^{\circ}\text{F}\cdot\text{day}$). This work emphasizes issues that can aid development of future guidelines for application of BEM and meter data to heat-wave scenarios.

INTRODUCTION

A heat wave is a prolonged period of abnormally hot weather. Global warming is shown to be tied to increasing magnitude, duration, and frequency of heat waves (Perkins, 2015; Horton et. al., 2016). The fifth Intergovernmental Panel on Climate Change (IPCC) report states that it is almost certain that heat wave risk will increase in the 21st century (IPCC, 2014). Heat waves cause death, damage, and infrastructure service complications and interruptions such as power outages (Santamouris, 2020; Falasca et. al, 2019; Burillo et. al., 2019; Santamouris et. al., 2015; Schubert et. al., 2014; Fennessy and Kinter, 2011). Air conditioning (AC) has reduced heat related deaths by a factor of six over the 20th century yet also is a contributor to anthropogenic global warming (Barreca et. al., 2013). AC is the dominant source of increased electricity demand during a heat wave (Choobineh et. al., 2019). In urban environments, heat rejection from AC systems can give positive feedback that elevates external ambient temperatures even further (Viguié et. al., 2020). Climatic heat waves coupled to this and other urban heat island effects are anticipated to create temperatures of $14\text{ }^{\circ}\text{C}$

Daniel L. Villa is a Senior Member of Technical Staff at Sandia National Laboratories, Albuquerque, NM

(25°F) higher than average peak temperatures (Santamouris, 2020).

Resilience to heat wave events can be obtained by several approaches. From the grid electricity supply side, power production and grid infrastructure can be bolstered such that maximum potential peak electrical loads can be serviced and maximum temperatures survived without concern. From the demand side, grid interactive buildings and passive cooling strategies (Baniassadi et. al., 2019) can be used to reduce demand or increase likelihood of survival for occupants during a heat wave. Unfortunately, all of these approaches are costly and correlations between designing for resilience to heat waves and designing for energy efficiency are not always positive (Sun et. al., 2020). As a result, quantification of heat wave effects on electric demand loads is of paramount importance so that risk for a given location can be assessed. Heat loads to be rejected by AC must therefore also be modeled. Building Energy Modeling (BEM) is a good method to do this.

Institutions that manage 10's-1000's of buildings with critical operations such as government entities, health care facilities, and universities are increasingly in need of ways to quantify the effects of heat waves on their infrastructure. Such quantification involves complicated analyses that must include uncertainty due to the need to incorporate downscaled climate modeling results. Methodologies are therefore needed that provide the uncertainty information needed while keeping complexity in the analysis to a minimum.

Sandia National Laboratories (SNL) conducted a heat wave analysis of its New Mexico site which has over 700 buildings with floor area of approximately 600,000 m² (6.5e6 ft²). The resulting analysis (Villa, 2020) led to the formulation of a procedure that uses BEM, a 2-parameter scaling function, and meter data to create two linear regressions of: 1) maximum heat wave temperature versus site-wide peak load and 2) heat wave heat content versus increased site energy consumption. The analysis created the linear regression models with 95% confidence intervals (CI) that represent uncertainty for: 1) operational variations within the buildings and 2) uncertainty in calculating site-wide peak loads when only partial metering is available. The second uncertainty had to be included because no direct measurement of site-wide power at 15 minute intervals was available. Building meters with 15 minute data only represented 69% of the NM site-wide power on average. Monthly energy bills of the entire site were therefore used to estimate this uncertainty and to normalize the analysis result to site-wide levels.

The purpose of this paper is to emphasize the need for development of generalized methodologies in heat wave analyses using BEM. This is accomplished through discussion of a follow-on analysis of the much smaller SNL California (CA) Livermore site with about 60 buildings and floor area of approximately 80,000 m² (860,000 ft²). The procedure proposed by the author (Villa, 2020) that was supposed to be generalized had many steps that did not work or were unnecessary in the CA analysis. The underlying BEM results did not initially fit the site-wide electricity demand. As a result, each building had to be investigated against its own meter data. These comparisons revealed that the BEM and metering signals had very different shapes from each other. It also revealed that the connectivity between centralized chilled water loops were not correct in the models. As a result, individual building calibrations had to be carried out. In the end, 9 BEM were calibrated to the American Society of Heating and Refrigeration American Engineers (ASHRAE) Guideline 14 (G-14) (ASHRAE, 2014) to produce a reasonably good site-wide fit. Even so, peak loads for the model were still consistently lower than the meter data. Other changes include: 1) The meter data filtration process was different for CA versus NM and the classification using K-means clustering were not needed for the CA site.

This paper first lays out a brief review of the heat wave analysis procedure from (Villa, 2020) with minor changes implemented for the CA site, presents the CA analysis results, and then briefly discusses lessons learned for generalized heat wave analysis procedures using BEM.

METHODS

The two parameter function used for the NM analysis (Villa, 2020) did not produce good fits between the CA BEM models and the data. A third parameter p_t therefore had to be added. The calibration function now provides scaling (p_m), stretching (p_o), and translation (p_t).

$$f_{new}(t, p_o, p_m, p_t) = \begin{cases} p_m[(1 - p_o)f(t) + f_{max}p_o] + p_t & 1 \geq p_o \geq 0 \\ p_m[-p_o f_{new-1}(t) + (p_o + 1)f(t)] + p_t & -1 \leq p_o < 0 \end{cases} \quad (1)$$

$$f_{new-1}(t) = \frac{f_{max}}{f_{max} - f_{min}} f(t) - \frac{f_{max}f_{min}}{f_{max} - f_{min}} \quad (2)$$

Here, $f(t)$ is the output for each time step simulated by the aggregate output of BEM, $f_{max} = \max(f(t))$, and $f_{min} = \min(f(t))$. The output calibration function $f_{new}(t)$ is compared to meter data $f_m(t)$ through the Normalized Mean Bias Error (NMBE) and Coefficient of Variation for Root Mean Square Error (CVRSME) as defined in G-14 (ASHRAE, 2014). The effects of p_m , p_o , and p_t are illustrated in Figure 1. The offset parameter p_o is less intuitive. It has a range of -1 to 1. At -1 it makes $f_{min} = 0$. At 1 it makes $f(t) = f_{max}$ for all t .

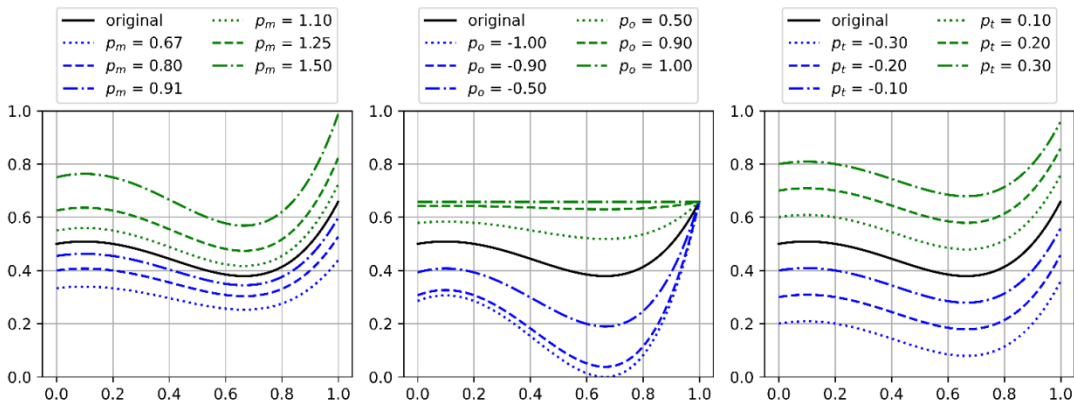


Figure 1 Parameter effects plots for p_m (left), p_o (middle), and p_t (right) for a random example function $f(t) = t(t + 1)(t - 0.9)(t - 0.2) + 0.5$

The procedure for running a heat wave analysis is shown in Figure 2 and is elaborated in more detail in (Villa, 2020). To conduct the analysis, the following input data is needed: 1) Energy meter data for the most recent year. This can be at the building level or for a site-wide meter. It is ideal to have 15 minute data for the entire site. 2) Hourly weather data for the the same year for inputs to BEM weather files. It is critical to use measured data for the site so that the BEM calibration fits to site performance. 3) Downscaled climate model results providing projected temperature histories into the future. 4) If site-wide meter 15 min data is unavailable monthly energy use bills for calculating normalization factors.

With these inputs, the heat wave analysis is accomplished according to the flow diagram in Figure 2 by: 1) Filtering the meter data for outliers and unphysical changes using Interquartile range (IQR), maximum rate of change, and aggregation to an hourly time step. 2) Calibration of invididual BEM models. 3) Deriving the heat wave start time during the year t_{hw} , change in peak temperature from the baseline peak temperature ΔT_{hw} , and length of the heat wave Δt_{hw} . 4) Removing time steps where the site is not in full operation. This is done through adjustment of input parameters to a K-means clustering algorithm followed by visual inspection of the model to data result for all time steps and for daily peak load. 5) Run all BEM using the IX software platform (Villa, 2017) or other platform. The BEM results then have to be scaled by minimizing the sum of the absolute value of NMBE and the CVRSME while varying p_m , p_o , and p_t . 6) Application of the heat wave in a discreet set of steps where the maximum temperature is offset to a fraction of ΔT_{hw} . Simulating several steps in IX provides a way to regress peak load versus maximum temperature from the BEM model results. 7) Calculate linear regressions of maximum temperature versus peak load and heat wave heat content versus increase in site-wide energy. 8) From step 1 and the weather data, develop a second dataset of maximum temperature versus peak load from the meter data. 9) Create a log-linear regression of peak load versus peak temperature with 95% confidence bounds of the maximum temperature. 10) Extrapolate the 95% confidence bounds from the log-linear

regression calculated in step 9 to the maximum heat wave temperature. This interval is the uncertainty in peak load due to operational variations. 11) Scale the meter results to site-wide results. This step was not needed for CA but was important to the NM case (Villa, 2020). 12) The outputs can then be provided with regression parameters with CI's. Estimations of the effect of different heat waves than the one simulated with estimated CI's can be made using the regression parameters, and calculation of t_{hw} , ΔT_{hw} , and Δt_{hw} for the heat wave in question.

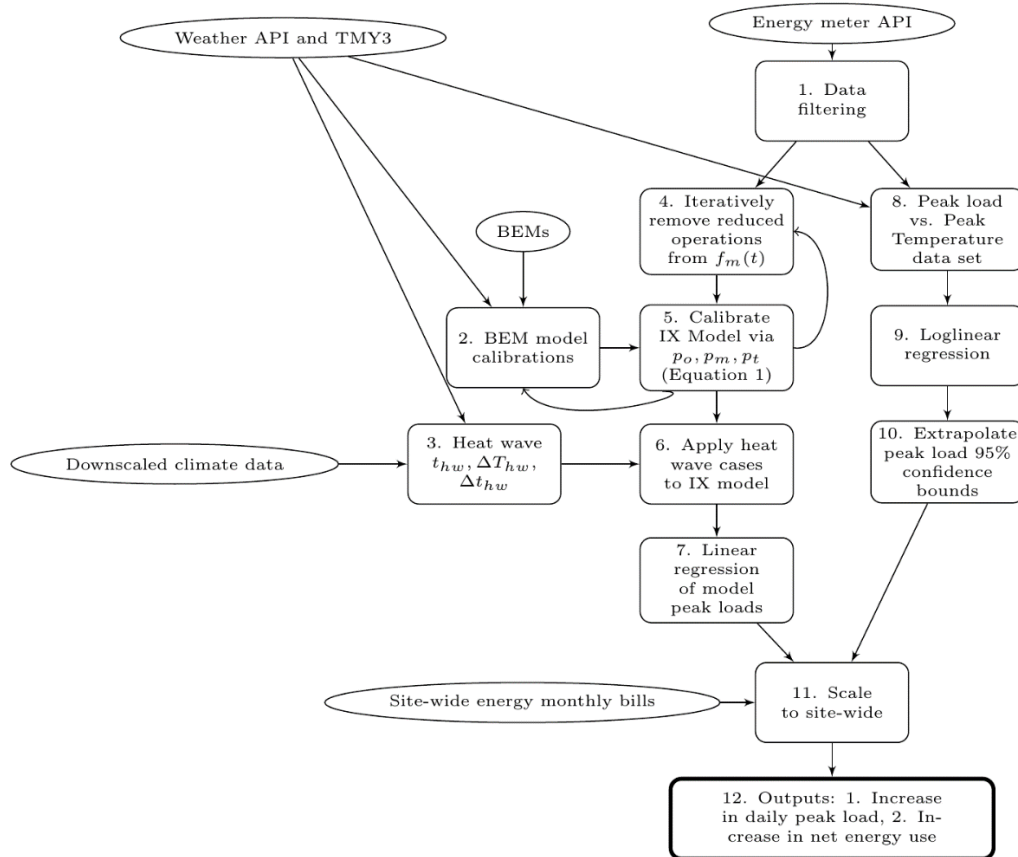


Figure 2 BEM heat-wave analysis procedure from (Villa, 2020) with modifications. Institutional Transformation (IX) is the BEM parameter study software platform used in this study

DATA INPUT

Weather data came from the Lawrence Livermore National Laboratory (LLNL) weather stations at 10 m elevation above ground level (LLNL, 2020) directly adjacent to the SNL CA site. The sensors used to collect the information are maintained, replaced and calibrated per Department of Energy (DOE) standards (DOE, 2015). The only non-available signals were total horizontal solar radiation, cloud type, and cloud amount. Typical Meteorological Year 3 (TMY3) data were used for these variables (Wilcox and Marion, 2008).

The meter data came from a site-wide electric meter recorded in the SNL energy analytics database. The data was extracted through a web application programming interface using Python. The accuracy of the meter was verified to be 0.32% variation between the yearly sum of energy between 2019 monthly bills and the 15 min meter data.

The heat wave scenario for CA was constructed from NEX-DCP30 model results (Thrasher et. al., 2013). The process to derive the heat wave is not elaborated here and is not critical because of the use of regression in this study to parameterize the heat wave. The total change in temperature was set to $\Delta T_{hw} = 3.4^{\circ}\text{C}$. The baseline hot period from the NEX-DCP30 historical results was chosen to be August 27th, 2017 ($t_{hw} = \text{August 27}^{\text{th}}$ each year) and the heat wave

was assumed to be 7 days long ($\Delta t_{hw} = 7$). Unlike the NM case, the 2°C volatility was not used due to lack of information about CA concerning increased volatility. The resulting scenario peak temperature of 45.1°C did not even break the current record high at the LLNL tower of 46.1°C , yet is still representative of expected, longer-duration future heat waves according to NEX-DCP30 model results.

RESULTS

The CA analysis required significant changes to the parameters of the analysis in comparison to the NM analysis. In step 1 (Figure 2) The IQR had to be expanded to 0.05 to 0.95 in comparison to the NM values of 0.1 to 0.9 to avoid shaving off some of the most prominent peaks for the CA data. Also, the K-means clustering that was essential to the NM analysis was not needed because non-full operations were not identified.

Performance of the institutional BEM heat wave analysis procedure required individual calibration of many of the BEM (step 2). While the NM site BEM (Villa, 2020) were under continuous maintenance (Villa, 2019), it appears that many of the CA building BEM had not recently been compared to meter data. Table 1 shows the NMSE and CVRSME of each of the 23 buildings before and after six iterations of manually changing the BEM that were guided by the capacity of the aggregate model response to match meter data peak loads in 2019 (Figure 5). The results of the iterative process between steps 2, 4, and 5 are shown in Figure 3. Figure 3b shows the IX model output for 23 BEM with no individual model calibration. Figure 3d shows the same result with the scaling function (Equation 1) applied. The model output gives G-14 compliant results but peak loads were clearly not modeled well. Figure 3f shows the model with removed data (orange). Unlike the NM case, the filtering process did not improve the fit to peak loads. Mismatch of peak loads is depicted in Figure 3f by light purple. The left column of Figure 3 shows the results after individual model calibration. Two major changes were needed for the scaling function to fit the meter data: 1) The AC energy needed to increase and 2) the reduction of loads at night and on weekends needed to be decreased significantly.

Investigation on a model by model basis, found that the day to night variation in plug, light, fan, and venting loads in the models were significantly too high in comparison to the data. Also, it was found that two major Central Utility Buildings (CUB) were not defined correctly across a group of 3 buildings and another group of 4 buildings. All 7 of these buildings were found to artificially meet their cooling loads with no electricity because they had previously been connected together into 2 models instead of 7. It was also found that all of the schedules within the models assumed significantly larger reductions in plug loads than actually occur according to the meter data. Figure 3a shows the updated aggregate output with no scaling. Figure 3c shows the unfiltered results scaled and Figure 3e shows the filtered result used for regression analysis. Even though the individual BEM calibrations produced much better peak loads, Figure 3e still shows the BEM underpredicting peak loads. The light purple peaks in Figure 3e consistently are higher than the 23 BEM model (dark purple or blue). This is clearly seen by observing the upper right hand corner of Figure 5.

The linear and data-driven log-linear regressions for peak load and site-wide energy created in Steps 6, 7, 9, and 10 are shown in Figure 4 and Figure 6. CI data and conversion to percentiles for these regressions are supplied in Table 2 and Table 3. These results provide the needed information to estimate other heat wave effects with CI's.

DISCUSSION

The CA site sensitivity is higher than the NM site (Villa, 2020). The less intense heat wave for CA ($28.10^{\circ}\text{C}\cdot\text{day}$ ($50.58^{\circ}\text{F}\cdot\text{day}$) versus $38.04^{\circ}\text{C}\cdot\text{day}$ ($68.47^{\circ}\text{F}\cdot\text{day}$) for NM) produced a $1.07\%/\text{ }^{\circ}\text{C}$ ($0.59\%/\text{ }^{\circ}\text{F}$) peak load sensitivity for the “work days” (last row of Table 3) prediction in comparison to NM's $0.67\%/\text{ }^{\circ}\text{C}$ ($0.37\%/\text{ }^{\circ}\text{F}$). Also, the energy sensitivity (Figure 6 and Table 2) is more uncertain for CA than NM. For peak load, the CA analysis has clear misalignment (Figure 4) between slope and offset. The inability to capture the higher peak loads with the 23 BEM models (Figure 5) despite changing AC systems to lower efficiencies indicates that there are unknown air-exchange, refrigeration, or heat loads in the 23 buildings being modeled. A better fit was not sought because the cause of mismatch could not be reasonably postulated from the information available. This points to the need for an objective criterion to compare peak loads.

The need for individual BEM calibration in this study increased the work-load required to assess the effects of heat

waves to the CA site. The combination of higher uncertainty obtained from the analysis results and increased work for the analysis suggests that follow on work should look at the effectiveness of using a low-resolution resistance capacitive (5RC1) BEM model (Bacher et. al., 2011; Madsen and Holst, 1995) to see if equivalent or better results can be obtained with less effort. Regardless, Table 1 shows that 9 of the detailed BEM used in this study became G-14 compliant. The production of G-14 compliant models has significant benefit to parallel modeling efforts to perform energy retrofit analyses using the BEM. This makes the time spent on this heat wave assessment more useful and shows an up-side to maintaining large fleets of BEM (Villa, 2019).

Table 1 Summary of individual building calibrations results.

	NMBE (%) Calibrated	NMBE (%) Uncalibrated	CVRSM (%) Calibrated	CVRSM (%) Uncalibrated	Data Mean Power (kW)	Model Mean Power Calibrated (kBTU/h)	Model Mean Power Uncalibrated (kW)	UnCalibrated (kBTU/h)
1	-3414	-5209	4.228E+04	4.26E+04	1.013	3.458	35.6	121.5
2	-5.5	11.41	206.7	206.7	225.3	768.8	237.7	811
3	92.86	87.31	101.9	97.15	193.4	659.9	13.83	47.17
4*	8.967	17.57	11.05	21.1	488.4	1667	444.6	1517
5*	-0.7239	37.61	23.05	45.59	37.98	129.6	38.25	130.5
6	-474	-178.6	476.9	226.6	102.7	350.3	589.3	2011
7*	0.6584	51.78	7.819	56.5	593.2	2024	589.3	2011
8*	0.6287	-8.661	17.98	81.37	101.6	346.7	101	344.5
9*	0.4323	-3.088	25.85	35.3	420.1	1433	418.3	1427
10	-191.6	-260.1	198.1	282.5	106	361.7	309.1	1055
11	-44.67	-78.66	69.07	105.9	213.7	729.1	309.1	1055
12*	-0.2531	-49.1	23.21	99.81	21.09	71.96	21.14	72.14
13	-18.89	31.5	42.31	49.83	31.95	109	37.98	129.6
14	-90.59	-93.12	147.9	190.1	15.07	51.42	28.72	98
15	-98.79	-192.5	163	310.9	16.69	56.96	33.19	113.2
16	-116.7	-120.6	170.5	162.3	70.1	239.2	151.9	518.3
17	-42.3	-41.2	51.58	111.2	118	402.6	167.9	572.8
18	0.1673	77.76	57.42	97.75	129.7	442.5	129.5	441.8
19	24.57	24.57	61.26	61.26	32.91	112.3	24.82	84.69
20	27.77	27.77	48.57	48.57	14.73	50.25	10.64	36.3
21*	-1.07	47.08	14.6	58.97	36.19	123.5	36.58	124.8
22*	-1.371	-43.79	18.49	60.07	110.1	375.7	111.6	380.9
23*	-2.128	31.99	27.39	47.27	90.29	308.1	92.22	314.7
Unscaled total	27.38	35.9	27.91	40.4		3059	1.044E+04	2700
Scaled total all data	2.563E-08	3.006E-07	5.242	7.202	4213	1.437E+04	4213	1.437E+04
Scaled total filtered data	4.418E-08	1.469E-08	5.121	6.74	4213	1.437E+04	4231	1.444E+04
								4236
								1.445E+04

* BEM that were G-14 compliant (NMBE < 10, CVRSME < 30) after calibration.

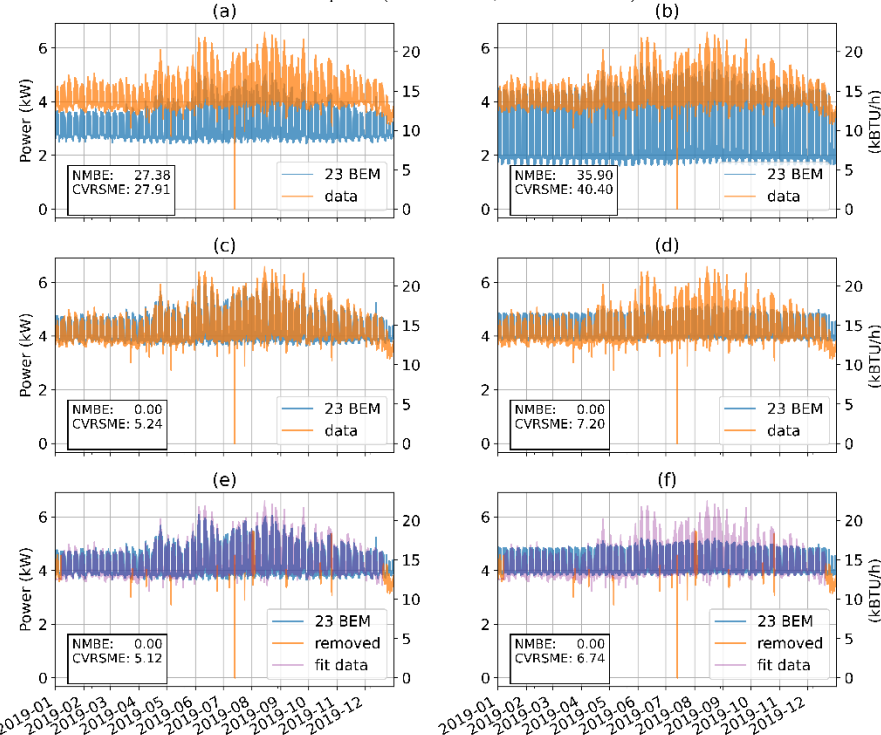


Figure 3 IX model with and without individual BEM calibration (a) Unscaled calibrated (b) Unscaled uncalibrated (c) Scaled calibrated no filtering (d) Scaled uncalibrated no filtering (e) Scaled calibrated with filtering (f) Scaled uncalibrated with filtering.

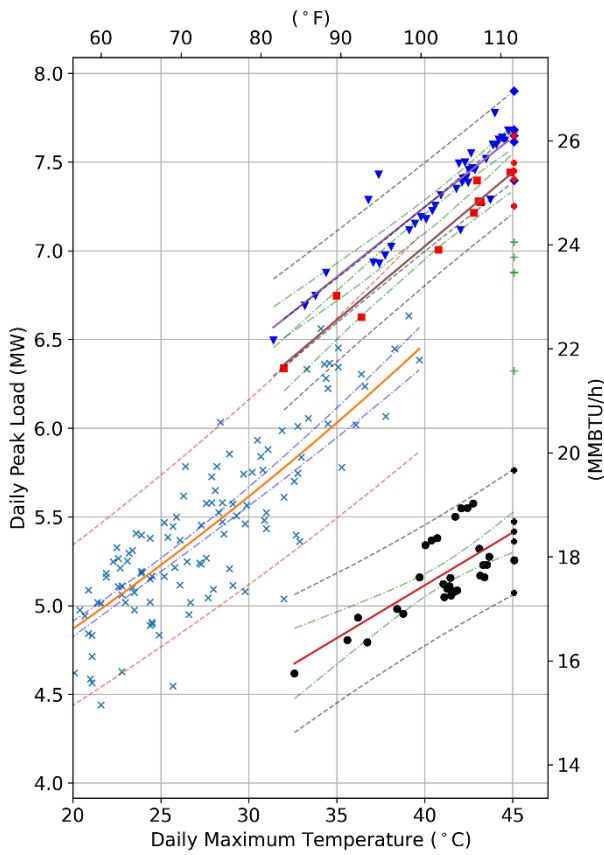


Figure 4 Regressions for peak loads

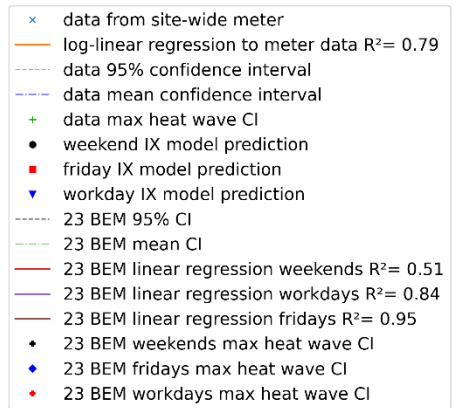


Figure 5 Data versus model peak load comparison

Care must be taken in interpreting CI's. CI's provide a statistical measure of the accuracy of calculations performed on the meter data but do not constitute a probability of occurrence of a given peak load. A statistical sampling study using the BEM and alternative weather histories would be needed to estimate probabilities.

CONCLUSION

An institutional heat-wave assessment has been performed at SNL CA that has shown that much more effort is needed when BEM have to be calibrated individually. A previous SNL NM analysis (Villa, 2020) required much less work because no individual BEM calibrations were needed to match site-wide meter data well. Other issues also arose for the SNL CA case: 1) The analysis procedure had to use an updated scaling function (Equation 1) with a translational parameter p_t ; 2) The classification filtering processes that were invaluable to the NM process did not add significant value to the CA analysis; and 3) The resulting CA uncertainty ranges were much wider than the NM analysis including inability to match the highest peak loads without direct investigation of the buildings involved. Future work needs to continue to refine this institutional BEM heat-wave assessment methodology including investigating the ability of 5RC1 models to produce equivalent results to detailed BEM. This work underscores issues that can aid development of future guidelines for application of BEM and meter data to heat-waves. The disparity in usefulness of data filtering in the two studies points to the need for classification techniques to be generalized for institutional BEM heat wave assessments.

The above difficulties suggest that detailed BEM modeling is not always a good approach for heat wave assessments. Though the NM site analysis was compelling and models were maintained more thoroughly (Villa, 2019), the CA site analysis was more difficult. The best approach to use depends on the purposes of the analysis. If individual building performance in resilience analysis of the site under a heat wave is desired, then the detailed approach is needed. For the current analysis, using the data-driven modeling without BEM has nearly the same accuracy when projected (Figure 4).

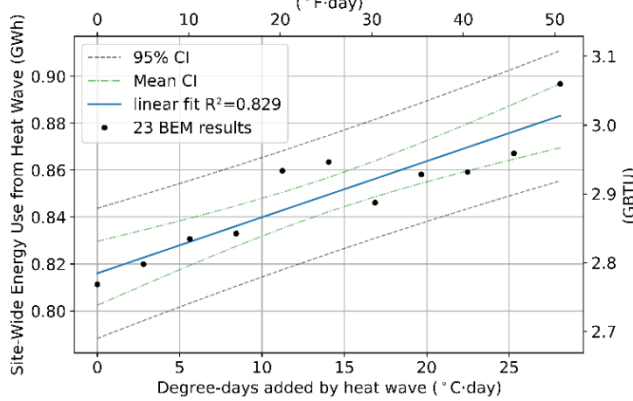


Figure 6 Site-wide energy-use due to heat waves

Table 2 Site-wide energy regression results

Description	Mean	+95% CI	-95% CI
Maximum heat wave 28.10°C-day (GWh)	0.8832	0.9109	0.8554
Maximum heat wave 50.59°F-day (GBTU)	3.014	3.108	2.919
Slope (GWh/°C-day)	0.002389	0.003209	0.00157
Slope (GBTU/°F-day)	0.004529	0.006083	0.002976
Intercept (GWh)	0.816	0.8297	0.8024
Intercept (GBTU)	2.784	2.831	2.738

Table 3 Peak load regression results

Description	Data (workdays)		Workdays		Fridays		Weekends	
	SI	English	SI	English	SI	English	SI	English
43.1°C mean predicted peak (MW/MMBTU)	6.962	23.76	7.647	26.09	7.448	25.42	5.417	18.48
— +95% CI	7.669	26.17	7.899	26.95	7.647	26.09	5.762	19.66
— +50% CI	7.049	24.05	7.68	26.2	7.494	25.57	5.473	18.67
— -50% CI	6.877	23.47	7.614	25.98	7.403	25.26	5.361	18.29
— -95% CI	6.321	21.57	7.395	25.23	7.25	24.74	5.072	17.31
37.2°C mean predicted peak (MW/MMBTU)	6.633	22.63	7.379	25.18	7.165	24.45	5.215	17.79
Heat wave to baseline % difference	4.965		3.631		3.949		3.879	
Mean slope (MW/°C or 1/°F) (MMBTU/°F or 1/°F)	0.01425*	0.007918*	0.07881	0.1494	0.08322	0.1578	0.0595	0.1128
— +95% CI	0.01539*	0.00855*	0.09057	0.1717	0.09958	0.1888	0.0823	0.156
— -95% CI	0.01312*	0.007286*	0.06706	0.1271	0.06687	0.1268	0.0823	0.156
Intercept (MW or unitless) (MMBTU or unitless)	8.205		4.093	13.96	3.695	12.61	2.733	9.327
— +95% intercept	8.234		4.572	15.6	4.355	14.86	3.668	12.51
— -95% intercept	8.177		3.614	12.33	3.035	10.36	1.799	6.14
R ² value	0.7929		0.837		0.9539		0.5051	
Model to data sensitivity % difference	0		-16.64		-11.97		-37.06	
Mean normalized slope (%/°C or %/°F)	1.46	0.8113	1.068	0.5934	1.161	0.6452	1.141	0.6339

* The data regression model was calculated as log-linear ($\ln(y/1 \text{ MW}) = ax + b$) or $\ln(y/1 \text{ MMBTU}) = ax + b$ where y is peak power in MW and x is daily maximum temperature. All others are for a linear model ($y = ax + b$).

This work must be tied to resilience assessments where effects on cost and infrastructure due to increases in energy use and peak load during a heat wave are quantified. The reduction of the BEM and data to regression parameters with CI's provides a low-order method with uncertainty for incorporating heat waves into energy master planning analyses (Jeffers, 2020) that consider additional forcing events such as human-attacks, earthquakes, floods, draughts, and fires.

DISCLAIMER

Sandia National Laboratories is a multimission laboratory managed and operated by National Technology and Engineering Solutions of Sandia, LLC., a wholly owned subsidiary of Honeywell International, Inc., for the U.S. Department of Energy's National Nuclear Security Administration under contract DE-NA0003525. This paper describes objective technical results and analysis. Any subjective views or opinions that might be expressed in the paper do not necessarily represent the views of the U.S. Department of Energy or the United States Government.

ACKNOWLEDGEMENTS

Thank you to Regina Deola, Gerald Gallegos, Nicole Rinaldi, and Robin Jones for championing this work and providing the NEX-DCP30 parameters for this analysis. Thanks for support from my wife Marina. Soli Deo Gloria et Christi.

REFERENCES

ASHRAE. 2014. ASHRAE Guideline 14-2014, "Measurement of Energy, Demand, and Water Savings." Atlanta: ASHRAE.

Baniassadi, Amir, David J. Sailor, and Harvey J. Bryan. 2019. "Effectiveness of phase change materials for improving the resiliency of residential buildings to extreme thermal conditions." *Solar Energy* 188: 190-199.

Bacher, Peder, and Henrik Madsen. 2011. "Identifying suitable models for the heat dynamics of buildings." *Energy and Buildings* 43(7): 1511-1522.

Barreca, Alan, Karen Clay, Olivier Deschênes, Michael Greenstone, and Joseph S. Shapiro. 2013. "Adapting to Climate Change: The Remarkable Decline in the U.S. Temperature-Mortality Relationship over the 20th Century." Massashussets Institute of Technology Working Paper CEEPR WP 2013-003. Cambridge, MA USA.

Burillo, Daniel, Mikhail V. Chester, Stephanie Pincetl, Eric D. Fournier, and Janet Reyna. 2019. "Forecasting peak electricity demand for Los Angeles considering higher air temperatures due to climate change." *Applied Energy* Vol. 236: 1-9.

Choobineh, Moein, Andrew Speake, Maxwell Harris, Paulo Cesar Tabares-Velasco, and Salman Mohagheghi. 2019. "End-User-Aware Community Energy Management in a Distribution System Exposed to Extreme Temperatures." *IEEE Transactions on Smart Grid* 10(4): 3753-3764.

DOE, 2015. "Environmental Radiological Effluent Monitoring and Environmental Surveillance." Department of Energy Handbook DOE-HNBK-1216-2015. <https://www.standards.doe.gov/standards-documents/1200/1216-bhdbk-2015>

Falasca, Serena, Virgilio Ciancio, Ferninando Salata, Iacopo Golasi, Federica Rosso, and Gabriele Curci. 2019. "High albedo materials to counteract heat waves in cities: An assessment of meteorology, building energy needs and pedestrian thermal comfort." *Building and Environment* 163:1-14.

Fennessy, M. J. and J. L. Kinter. 2011. "Climatic Feedbacks during the 2003 European Heat Wave." *Journal of Climate* 24(23): 5953-5967.

Horton, Radley M., Justin S. Mankin, Corey Lesk, Ethan Coffel, and Colin Raymond. 2016. "A Review of Recent Advances in Research on Extreme Heat Events." *Current Climate Change Reports* 2(4): 242-259.

IPCC, 2014. "Climate Change 2014: Synthesis Report. Contribution of Working Groups I, II, and III to the Fifth Assessment Report of the Intergovernmenatal Panel on Climate Change [Core Writing Team, R.K. Pachauri and L.A. Meyers (eds.)]. IPCC, Geneva Switzerland, 151 pp.

Jeffers, Robert, Amanda M. Wachtel, Alexander M. Zhivov, Calum B. Thompson, Avinash Srivastava, and Patrick W. Daniels. 2020. "Integration of resilience goals into energy master planning framework for communities." *ASHRAE Transactions* 126:803-823

LLNL, 2020. <https://weather.llnl.gov> Accessed 1/15/2020. For calibration standards see: <https://weather.llnl.gov/cgi-bin/about.pl>

Madsen, Henrik, and Jan Holst. 1995. "Estimation of continuous-time models for the heat dynamics of a building." *Energy and Buildings* 22(1): 67-79.

Perkins, Sarah E. 2015. "A review on the scientific understanding of heatwaves—Their measurement, driving mechanisms, and changes at the global scale." *Atmospheric Research* Vol. 164 Iss. 165: 242-267.

Santamouris, M., C. Cartalis, A. Synnefa, and D. Kolokotsa. 2015. "On the impact of urban heat island and global warming on the power demand and electricity consumption of buildings—A review." *Energy and Buildings* 98: 119-124.

Santamouris, M. 2020. "Recent progress on urban overheating and heat island research. Integrated assessment of the energy, environmental, vulnerability and health impact. Synergies with the global climate change." *Energy and Buildings* 207: 109482.

Schubert, Siegfried D., Hailan Wang, Randal D. Koster, Max J. Suarez, and Pavel Ya Groisman. 2014. "Northern Eurasian Heat Waves and Droughts." *Journal of Climate* 27(9): 3169-3207.

Sun, Kaiyu, Michael Specian, and Tianzen Hong. 2020. "Nexus of thermal resilience and energy efficiency in buildings: A case study of a nursing home." *Building and Environment* 177: 106842.

Thrasher, Bridget, Jun Xiong, Weile Wang, Forrest Melton, Andrew Michaelis, and Ramakrishna Nemani. 2013. "Downscaled climate projections suitable for resource management. *Eos, Transactions American Geophysical Union* 94(37): 321-323

Viguié, Vincent, Aude Lemonsu, Stéphane Hallegatte, Anne-Lise Beaulant, Colette Marchadier, Valéry Masson, Grégoire Pigeon and Jean-Luc Salagnac. 2020. "Early adaptation to heat waves and future reduction of air-conditioning energy use in Paris." *Environmental Research Letters* 15: 075006.

Villa, Daniel L., Jack H. Mizner, Howard D. Passell, Marlin S. Addison, Gerald R. Gallegos, William J. Peplinski, Douglas W. Vetter, Christopher A. Evans, Leonard A. Malczynski, Matthew A. Schaffer, and Matthew W. Higgins. 2017.

“Institutional Transformation Version 2.5 Modeling and Planning.” *Sandia National Laboratories Technical Report SAND2017-1498*. February.

Villa, Daniel L., Joshua R. New, Mark Adams, Aaron Garrett, and Gerald R. Gallegos. 2019. “First Steps to Maintain a Large Fleet of Building Energy Models.” *Conference Paper for the ASHRAE 2019 Summer Meeting*. Kansas City, MO. June.

Villa, Daniel. 2020. “Institutional Heat Wave Analysis by Building Energy Modeling Fleet and Meter Data.” *Submitted to Energy and Buildings but not yet accepted*.

Wilcox, S. and W. Marion. 2008. “User’s Manual for TMY3 Data Sets”. *National Renewable Energy Laboratory Technical Report NREL/TP-581-43156*. April.